TECHNICAL REPORT

Physical Features of Coastal Upwelling Systems

Robert L. Smith

WSG 83-2
April 1983

TECHNICAL REPORT

Physical Features of Coastal Upwelling Systems

Robert L. Smith

Washington Sea Grant Program
College of Ocean and Fishery Sciences
University of Washington HG-30
Seattle, Washington 98195

WSG 83-2
April 1983

Acknowledgments

I spent much of the decade of the 1970s doing research as part of the Coastal Upwelling Ecosystems Analysis project, supported by the National Science Foundation. In this paper, I have drawn liberally from some previous papers, especially Smith (1978 and 1981), and Barber and Smith (1981). The motivation to keep biology and fisheries in mind while considering the physical processes comes from Professors Ole A. Mathisen (University of Washington School of Fisheries and Dean, School of Fisheries and Science, University of Alaska, Juneau) and Richard T. Barber (Duke University Marine Laboratory).

About the Author

Robert Smith began studying upwelling off Oregon while doing graduate work at Oregon State University, where he received a Ph.D. in oceanography in 1964. He was a NATO Fellow in England, served as Scientific Officer with the Office of Naval Research in Washington, D.C., and was a visiting Professor at the Institut fur Meereskunde an der Universitat Kiel in Germany. He is now a professor of Oceanography at Oregon State University in Corvallis, Oregon.

Key Words

1. Coastal upwelling. 2. Upwelling-- in oceans 3. Ocean currents
4. Oceanography

Support for this publication is provided by grant NA81AA-D-00030, project AP/C-5 and E/F-4, from the National Oceanic and Atmospheric Administration to the Washington Sea Grant Program.

Washington Sea Grant Communications
College of Ocean and Fishery Sciences HG-30
Seattle, Washington 98195

WSG 83-2
April 1983

$3.50

Contents

Prologue

Among the oceanic phenomena affecting man, the rise of deeper water to the surface along the western coasts of Africa and the Americas has an especially direct impact on the social and economic fabric of his life. English speaking oceanographers refer to the phenomenon as coastal "upwelling"; the Spanish refer to it as "afloramiento," which appropriately sounds like it means "flowering" but simply means outcropping.

Figure 1 shows the major coastal upwellings regions. The figure is based on one from a National Science Board publication (1971) on which is superimposed the atmospheric high-pressure systems (anticyclones) that dominate the climatology of the regions (Thompson, 1977). Nearly 50 percent of the global commercial harvest of fish was estimated to come from coastal upwelling regions, which comprise less than one percent of the total area of the world ocean (Ryther, 1969). This heavy harvest is the result of a complex set of physical and biological processes that make up the coastal upwelling ecosystem. During the International Decade of Ocean Exploration (the 1970s) these processes were the object of concentrated study by European and American oceanographers in experiments off the west coast of North Africa, the Peruvian coast, and the west coast of North America. In this paper we will focus on the physical processes associated with coastal upwelling.

When one thinks of movement of water in the ocean, one tends to think only of horizontal motion: the rapid flow of the Gulf Stream and its eddies, weaker current systems that clearly affect both navigation and climate, and horizontal flow on a smaller scale that carries an oil spill, or a drifting raft, toward or away from beaches. The effects, indeed the existence, of vertical motion in the ocean is not nearly so apparent. This is not surprising since sustained vertical flow in the ocean is only 10^{-5} to 10^{-2} cm sec^{-1} (1 cm to 10 meters per day at most), while typical horizontal flow is 10 to more than 100 cm sec^{-1} (10 km to more than 100 km per day). This ratio of 1000 or more to 1 in favor of horizontal velocities is partly because the ocean is 1000 times as wide as it is deep, and partly because it is stratified, i.e., it has increasing density with depth resulting from decreasing temperature with depth. Density stratification tends to decrease vertical motion since energy must be used to displace water in a vertical direction—i.e., work must be done against gravity.

The consequences of small vertical components of velocity cannot be neglected because there exist large vertical gradients in the concentration of dissolved nutrients and gases as well as temperature and salinity. Even a small vertical

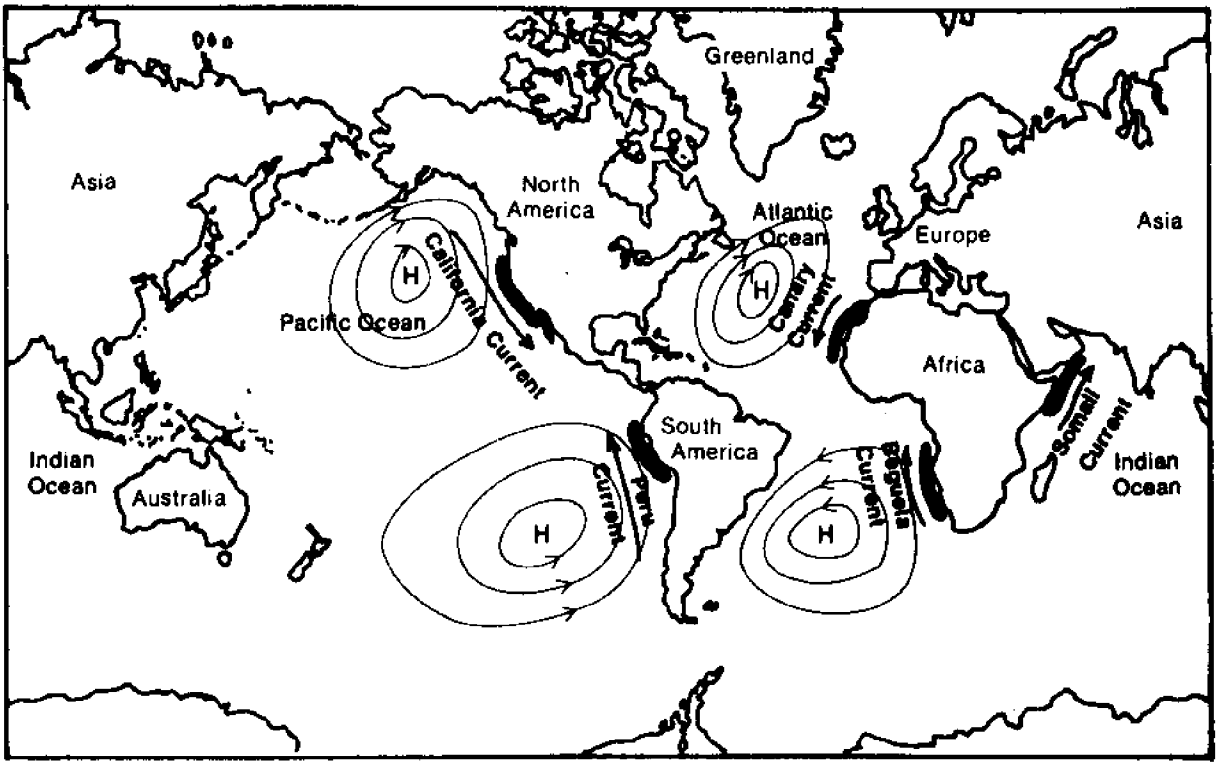

Figure 1. The major coastal upwelling regions and the summer positions of atmospheric high-pressure systems, i.e., anticyclones. Reference: National Science Board 1971 and Thompson, 1977.

component brings water with different characteristics from one level to another. Without this vertical motion the sea would be virtually lifeless. At the rate of primary production present in the ocean, depletion of nutrients from the surface (euphotic) layer would lead to a virtually lifeless sea in less than a year (Turekian, 1968). Therein lies the importance of vertical motion in the ocean.

Upwelling is, in general, the result of horizontal divergence in the flow of the surface layer and may occur anywhere. Although deep vertical mixing also occurs anywhere as a result of transient storms and leads to a replenishment of nutrients to the surface layer, the upwelling process in the coastal regions indicated in Figure 1 provides a more persistent supply of nutrients, which enables high biological productivity to persist.

Some Basic Physics

Major coastal upwelling regions are located along the eastern boundaries of the oceans, i.e., the west coasts of the continents. Along eastern boundaries the pool of nutrients does not lie very deep below the surface: for example, 100 km off Oregon (or Mauritania, in northwest Africa, or Peru) the concentration of nitrate (NO_3) might be only 0.03 milligrams per liter of water in the upper 10 m, but is more than 50 times greater (1.5 milligram/liter) at 100 m depth. Predominant winds along these coasts are part of the circulation around the quasi-stationary, mid-ocean, atmospheric high pressure systems (e.g., the North Pacific High and the Azores High in the eastern North Atlantic). The predominant wind is toward the Equator and nearly parallel to the coast in coastal upwelling regions.

The net effect of alongshore winds is to move the surface water *away* from the coast because of the effect of the earth's rotation. The earth's rotation gives rise to an apparent force, the Coriolis force, named after the French engineer and mathematician G.-G. de Coriolis who formalized the concept. To an observer on the rotating earth, any moving object is subjected to a "Coriolis acceleration" directed exactly at a right angle to its motion. The magnitude of the Coriolis force on a unit mass (acceleration) is proportional to the speed of the object (v) and the latitude (or more precisely, the Coriolis parameter f where $f = 2\Omega \sin \phi$ and Ω is the earth's angular velocity and ϕ the latitude). The Coriolis force per unit mass is fv. When wind blows over the ocean it exerts a force on the sea surface in the direction it is blowing, i.e., its momentum is transferred to the ocean, tending to drag the surface water with it. As soon as the water begins to move, it experiences both the Coriolis force and the force of the wind.

The resultant effect on ocean currents of the Coriolis force combined with wind forces was not adequately understood until the beginning of this century, and a brief historical and theoretical excursion is in order. During the drift of the arctic research ship FRAM across the polar sea in 1893-96, Norwegian explorer-oceanographer Fridtjof Nansen observed that the ice drift was at 20° to 40° to the right of the wind. He attributed this to the effect of the Coriolis force, and inferred that the water below, dragged along by the ice or water above, must be deflected even further to the right. Swedish theoretical physicist V. W. Ekman (1905), motivated by these observations, produced the theoretical explanation in a now classic paper. He assumed a balance existed between the Coriolis force and the frictional forces (frictional drag) resulting from turbulent transport of

momentum from the wind into the surface layer of the sea. Using a constant eddy viscosity and vertical shear of the horizontal flow to parameterize the turbulence process, the equations of motion for the assumed balance becomes (with u, v the eastward, northward currents):

$$o = fv + A \frac{\partial u}{\partial z^2}$$

$$o = -fu + A \frac{\partial^2 v}{\partial z^2}$$

A simple, elegant solution is obtained by requiring that wind stress, τ, (force per area) matches shear stress in the fluid at the surface. The surface boundary condition becomes (with τ_x, τ_y the eastward, northward wind stress components):

$$\tau_x = \rho A \frac{\partial u}{\partial z}\Big|_{z=0} \quad ; \quad \tau_y = \rho A \frac{\partial v}{\partial z}\Big|_{z=0}$$

where ρ is the water density and A the eddy viscosity. Typical values for A are of the order of 1 to 100 $cm^2\ sec^{-1}$. Velocities and velocity gradients are assumed to vanish at great depth.

The resulting surface velocity is 45^o to the right (left) of the wind direction in the Northern Hemisphere (Southern Hemisphere) and decreases exponentially with depth with the direction rotating to the right (left) with increasing depth. This logarithmic spiral is called the Ekman spiral. The surface speed is $\tau(fA\rho^2)^{-1/2}$ and has decreased by e^{-1} at $z = -(2A/f)^{1/2}$. The depth $(2A/f)^{1/2}$ is called the Ekman depth or depth of frictional influence, and the layer from the boundary to that depth is called the Ekman layer. The Ekman layer is some tens of meters thick, depending on stratification and wind intensity. An Ekman layer will occur along any boundary that exerts a frictional drag (e.g., wind stress or bottom friction) on the fluid.

A very important result, which is independent of eddy viscosity, can be obtained by integrating the above equations of motion with depth to obtain the net mass transport due to the wind:

$$M_x = \int_{z=-D}^{o} \rho u dz = \frac{\tau_y}{f}$$

$$M_y = \int_{z=-D}^{o} \rho v dz = -\frac{\tau_x}{f}$$

The lower limits of integration are formally indicated as -D, where D is some depth sufficiently great that the stresses (velocity gradients) vanish. D can be taken as approximately the Ekman depth, since the velocities decay exponentially.

Thus, net movement of water in the layer affected by wind, i.e., the Ekman layer, is at right angles to the wind (90^{o} to the right in the Northern Hemisphere, 90^{o} to the left in the Southern Hemisphere). The amount of water so moved by the wind is called the Ekman transport.

Quantitatively, the Ekman transport (the mass of water moved, in unit time, at right angles to the wind through a strip of unit width extending from the surface to below the Ekman depth) is equal to the wind stress (force per unit area exerted by the wind on the sea surface) divided by the Coriolis parameter f. Wind stress has the same direction as the wind, but is proportional to the square of the wind speed. The wind stress vector has the direction of the wind; its magnitude is approximately equal to the product of the air density, ρ_a, a dimensionless drag coefficient, $C_D = 1.5 \times 10^{-3}$, and the square of the wind speed:

$$\tau = \rho_a \, C_D \, ||v_{wind}|| v_{wind}$$

Hence the Ekman transport increases strongly with increasing wind.

A Simple Conceptual Model

When wind blows parallel to a coastline, an Ekman transport perpendicular to the coast (toward or away from the coast) is established. If the coastline is to the left, looking in the direction the wind is blowing, in the Northern Hemisphere (or to the right in the Southern Hemisphere), the Ekman transport is directed offshore (Figure 2). Near the coast, water can be supplied to feed offshore-directed Ekman transport only by drawing it up from below. As the surface water is swept offshore, an equal volume of deeper, and colder, water wells up to replace it near the coast. Thus the magnitude of the Ekman transport directed offshore, computed from the alongshore component of wind stress divided by the Coriolis parameter, is an index of the magnitude of coastal upwelling. This is exactly what Bakun (1973) computes as the Upwelling Index, which is disseminated by the National Marine Fisheries Service (NMFS) of NOAA.

If we look at sea surface temperature maps of the ocean we find confirmation of this effect, e.g., we can compare the difference between coastal sea surface temperatures and mid-ocean surface temperatures. Are coastal temperatures cooler where and when alongshore wind is such that the Ekman transport at the coast is directed offshore? Figure 3, based on research by Wooster et al. (1976), shows these comparisons for the eastern North Atlantic. The anomalously cold coastal temperatures at the coast (compared with mid-ocean surface temperatures at the same latitude) are caused by upwelling of deeper (and colder) water near the coast as wind transports surface water out to sea. Note the cold water off Portugal during summer, associated with increased offshore Ekman transport.

A very similar picture emerges on the west coast of the United States during summer (Figure 4). A vertical section of temperature, perpendicular to the coast, is instructive: the temperature and nitrate distributions in a vertical section extending off the Oregon coast in July 1968 are shown in Figure 5. Winds are generally favorable (blowing from the north) for upwelling from April through

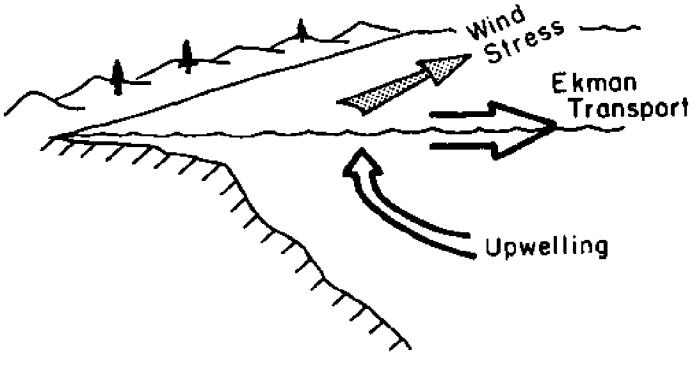

Figure 2. A conceptual diagram of the coastal upwelling process. The west coast of a continent in the Northern Hemisphere is shown with wind blowing from the north. Offshore transport in the surface Ekman layer results from wind parallel to the coast; water moving offshore in the surface layer must be replaced by upwelling from deeper water.

September along the Northern California, Oregon, and Washington coasts. For two weeks prior to the 1968 observations the wind was strongly favorable for upwelling and the effects of coastal upwelling were seen in the rise of deeper water toward the coast. It was apparent that the direct effect of upwelling, and presumably the vertical transport of deep, colder, and nutrient-rich water was occurring within 30 km of the coast.

The conditions shown in Figure 5 are consistent with the theory (Charney, 1955; Yoshida, 1955) of response of stratified rotating fluids to forcing near a boundary. Theory suggests that upwelling, or replacement of water moved offshore as the Ekman transport, would occur within a coastal zone with an offshore scale given by the "baroclinic radius of deformation," which is estimated by the equation

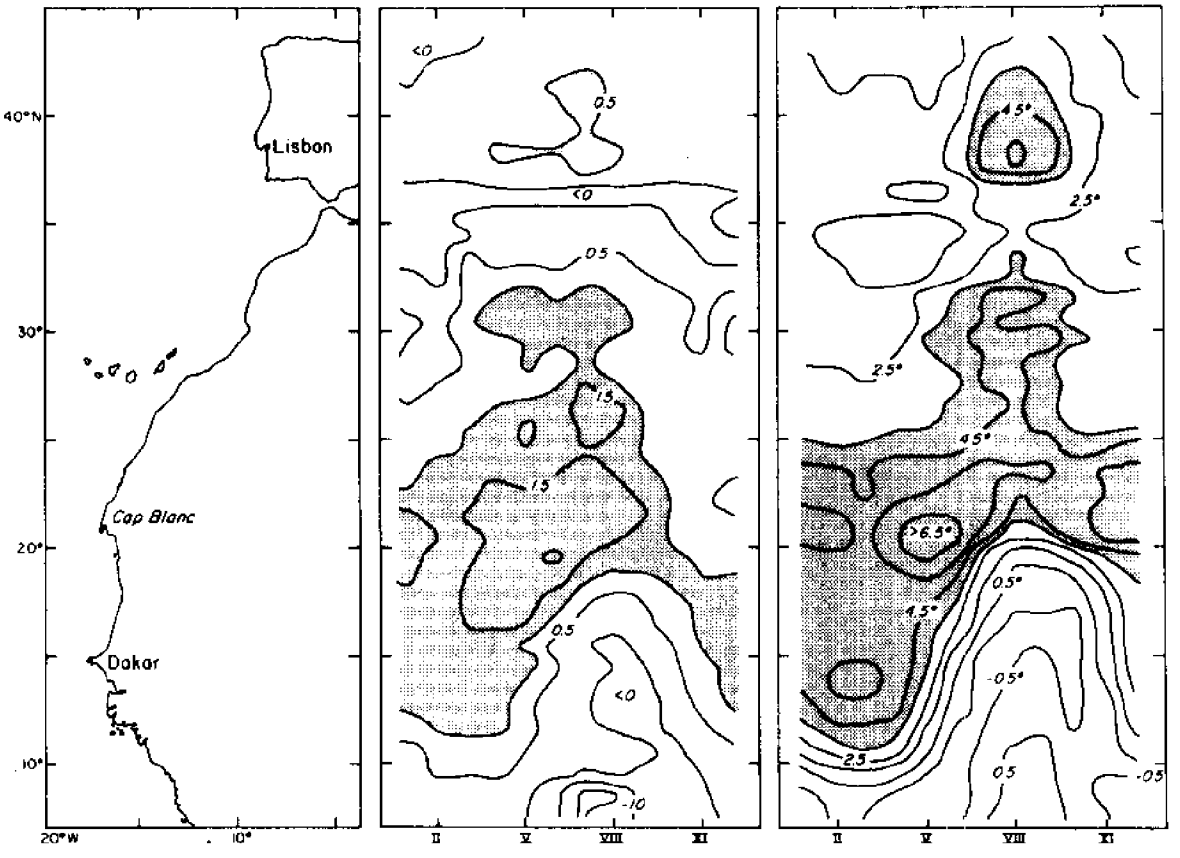

Figure 3. a) The west coast of the Iberian peninsula and northwest Africa, where the wind blows with a component from the north during much of the year. b) Ekman transport near the coast computed from the alongshore component of wind stress. The data is plotted against latitude (vertical axis) and month (horizontal axis). Positive numbers, mean surface flow directed offshore, and shaded areas represent relative maxima in the offshore Ekman transport. The units of transport are $m^3 s^{-1}$ per meter of coastline. c) The difference between mid-ocean and coastal sea surface temperatures in $^{\circ}C$, plotted in the same manner as the Ekman transport in b). Positive values indicate coastal temperatures colder than mid-ocean. Shaded areas represent coastal temperatures colder by $3.5^{\circ}C$ or more than mid-ocean surface temperatures. Source: Wooster et al., 1976.

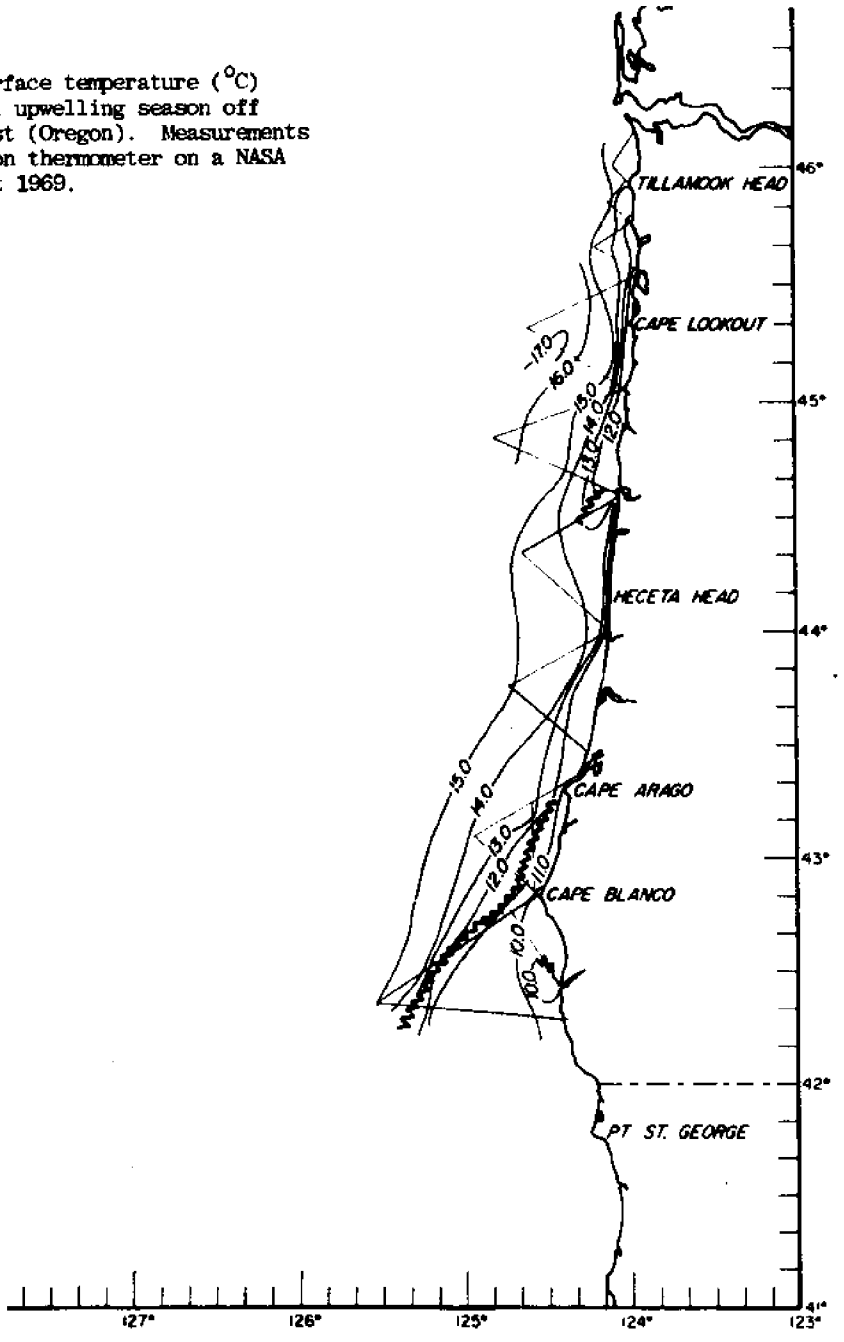

Figure 4. Sea surface temperature (°C) during the coastal upwelling season off the U.S. west coast (Oregon). Measurements made with radiation thermometer on a NASA aircraft, 12 August 1969.

R = HN/f. The relevant parameters for giving the width of a coastal boundary process are thus the average vertical density gradient ($N^2 = \frac{g}{\rho}\frac{\partial \rho}{\partial z}$ where g is gravitational acceleration and ρ the water density), the water depth H, and the Coriolis parameter (i.e., latitude). For Oregon, R is on the order of 15 km, and we see that the nutrients from below 100 m are reaching the surface within 15 km of the coast. The source water for coastal upwelling is seldom greater than a couple of hundred meters, and is usually less. Off Oregon and northwest Africa, the upwelling water near the coast comes from an offshore depth of 100 to 200 m; but off Peru, the source depth is usually 50 to 75 m (Figure 6).

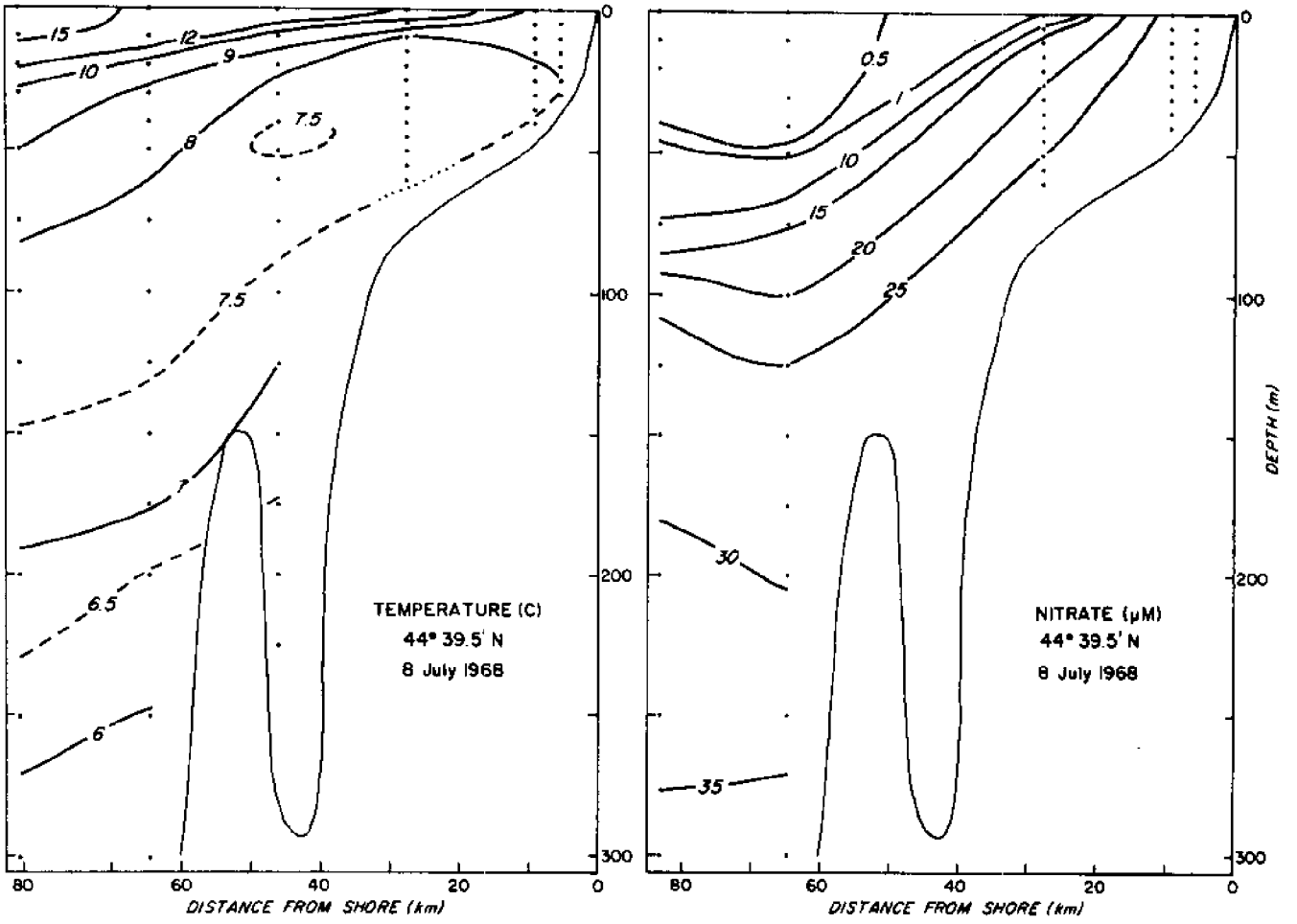

Figure 5. Temperature and nitrate distributions in a cross section extending off the Oregon coast during coastal upwelling. The concentration of nitrate is given in micro-molar units (μM). A concentration of 1 μM is equivalent to 62 micrograms of nitrate per liter of sea water. The deep upwelled water is very rich in nitrate by ocean standards (1.5 milligrams per liter), although not by the standards of terrestrial farmers.

The rise of denser water toward the coast changes the internal density distribution, and hence the internal pressure field. Since cold upwelling water is much denser than the surface water it displaces, it must be actively lifted by some mechanical force. This force is supplied by a pressure drop at the coast, which arises as the offshore Ekman drift begins. Since water cannot flow through the coastline, the sea surface level is lowered at the coast, causing a shoreward pressure gradient to form in the entire water column below.

Near the surface, this pressure gradient inhibits the veering of the wind-accelerated surface waters, and the acceleration proceeds until an alongshore current develops where the Coriolis force balances the coastward pressure drop, i.e., a geostrophic balance is attained (see Stommel, 1960, pp. 16-21, for an excellent brief discussion of the geostrophic balance). Figure 7, shows the alongshore flow that developed off Oregon after several weeks of upwelling

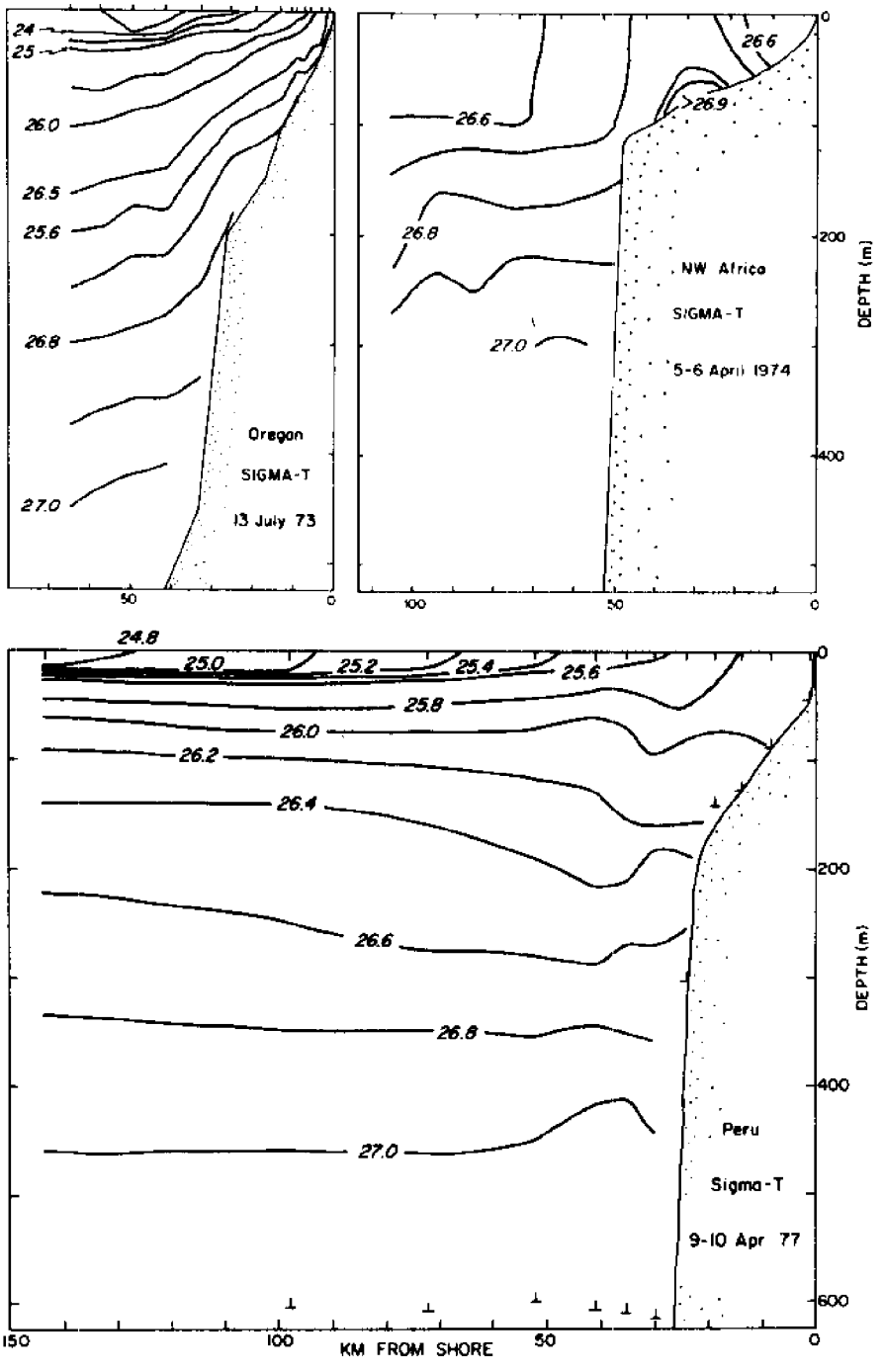

Figure 6. Cross-shelf density profiles from Oregon, northwest Africa, and Peru during upwelling-favorable winds.

favorable winds (Mooers, Collins, and Smith, 1976). An alongshore coastal jet developed in the direction of the wind where the horizontal density gradient—hence pressure gradient—was greatest. Once this alongshore flow pattern was established, the balance did not depend crucially on the surface wind. Therefore, if the wind suddenly stopped, the coastal current would continue its strong alongshore flow and the strong temperature gradient between the cold coastal water and warmer offshore water would be maintained. It usually takes a wind reversal to break this down by destroying the coastal jet and by setting up an onshore Ekman drift of warm water. Otherwise, only lateral mixing, perhaps by strong offshore

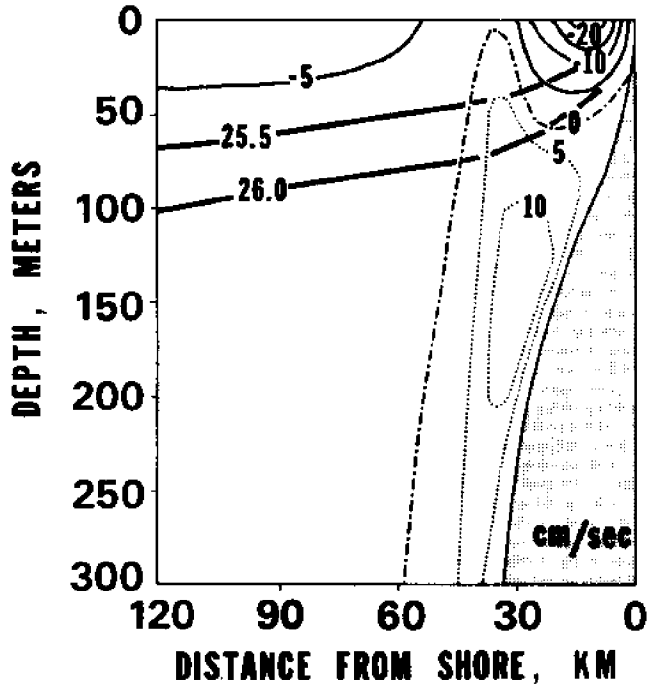

Figure 7. The flow parallel to the coast (i.e., the alongshore velocity) off Oregon during coastal upwelling. The wind is from the north, i.e., blowing southward. Solid lines and negative numbers indicate southward flow in the water—the coastal jet has speeds in excess of 10 cm sec^{-1}; dashed lines and positive numbers indicate northward flow—a poleward flowing undercurrent.

Heavy solid lines represent isopycnals (equal density surfaces) of 1.0255 and 1.0260 g cm^{-3}, roughly equivalent to temperatures of 9°C and 7.5°C respectively. Flow perpendicular to the coast is as indicated in Figure 2. Offshore flow (in the Ekman layer) is limited to about 25 m, the onshore flow that feeds the coastal upwelling process is present immediately beneath the surface Ekman layer. Source: Mooers, Collins, and Smith, 1976.

eddies, or the heat of the sun can act to eliminate the cold coastal condition after the upwelling favorable winds subside.

Note in Figure 7 another ubiquitous, but subsurface, feature of major coastal upwelling regions: a poleward flowing undercurrent, flowing opposite to the wind and the near surface flow. This undercurrent hugs the continental slope off the upwelling coasts of the Americas and Africa, sometimes extending onto the continental shelf, as is seen off Washington (in Figure 8; Hickey, 1979), northwest Africa (in Figure 9; Mittelstaedt et al., 1975), and Peru (in Figure 10; Brockmann et al., 1980). Although theories have been advanced to explain this phenomenon, there is no completely satisfactory physical explanation for it. Its importance to the ecology is more apparent. Consider that high primary productivity occurs near the surface in waters that move downwind (equatorward) and offshore. The detritus from high productivity, and from the higher trophic levels that it supports, sink out of the euphotic zone to deeper water, where inorganic nutrients gradually are regenerated by bacterial action. The undercurrent lying below the region of highest productivity transports the detrital products and nutrients back upstream. Thus a natural feedback process is established: the nutrients may be returned to the euphotic zone by onshore flow (compensating for the offshore Ekman transport above) and upwelled, to repeat the cycle. One can imagine that the biota itself may take advantage of this conveyer belt, thus remaining in regions of high productivity.

Figure 8. Alongshore currents off southern Washington, 21 July to 28 August 1972. Equatorward flow is shaded, speeds (right hand number) are cm s^{-1}; correlation (left hand number) with midshelf 66 m current record is shown; temperature field is indicated (numbers near left edge) in °C. Source: Hickey, 1979.

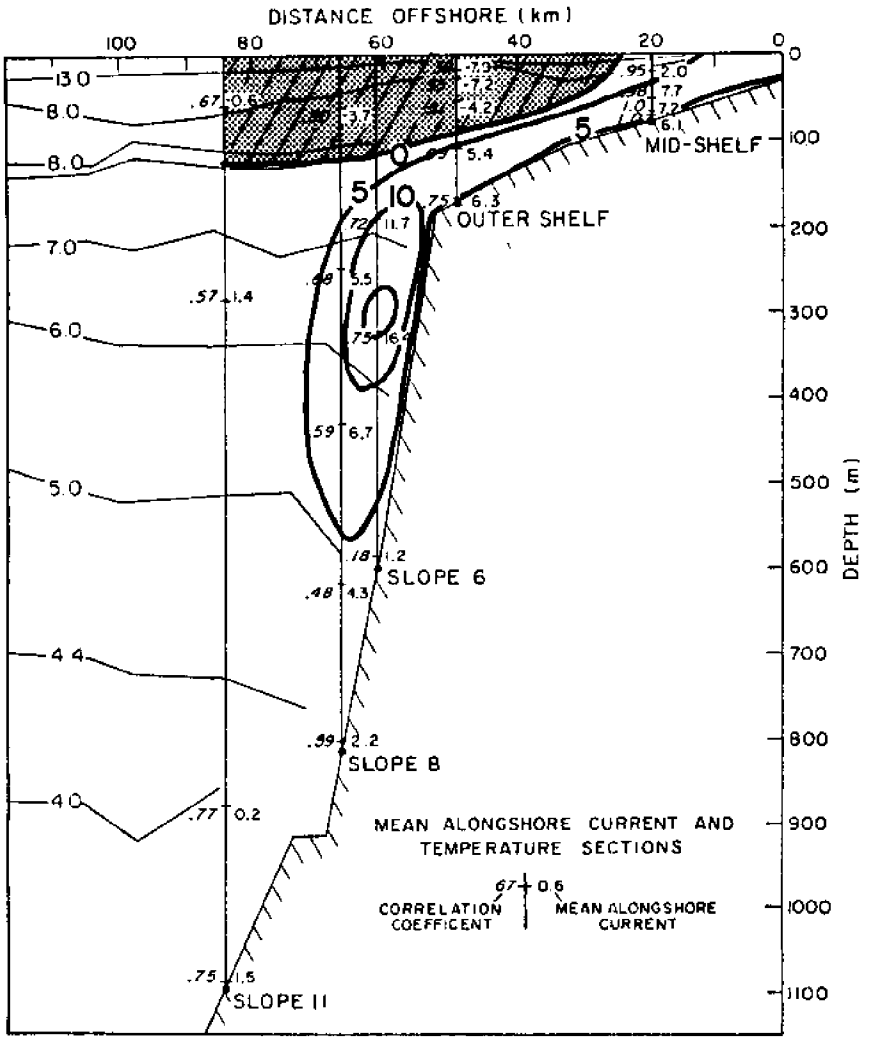

Figure 10. Alongshore currents at two latitudes off Peru, 2 April-10 May 1977. Poleward flow has negative sign and is shaded, speeds are cm s^{-1}. Equatorward flow has not been contoured. Source: Brockmann et al., 1980.

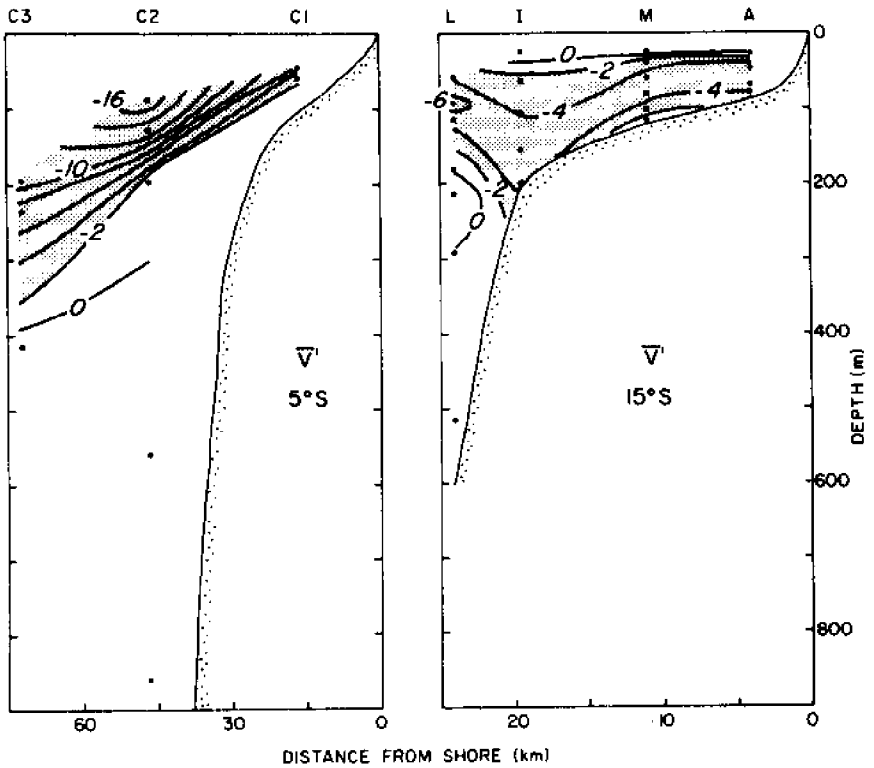

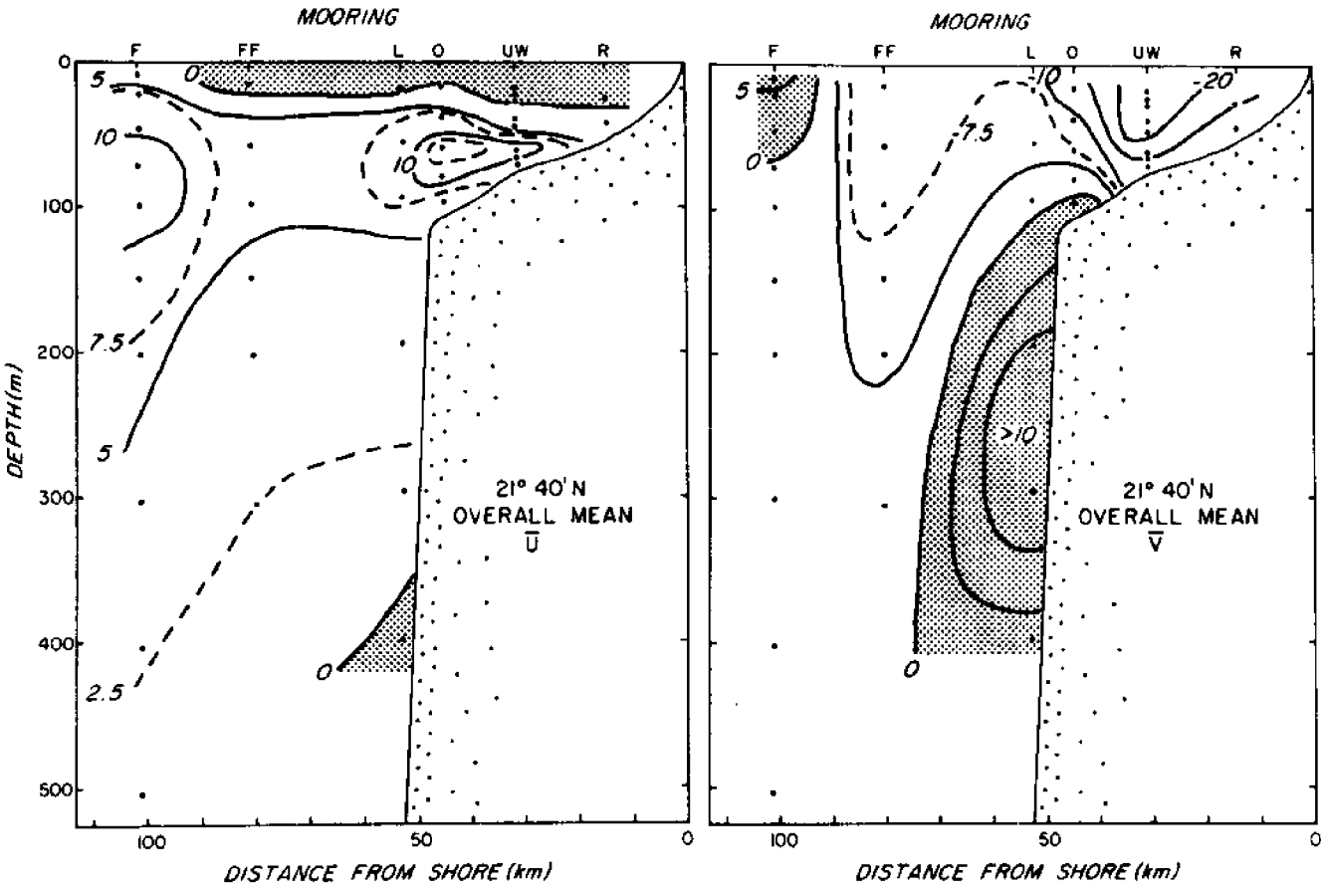

Figure 9. Mean onshore (U) and alongshore (V) currents off northwest Africa (21°40'N), February-April 1974. Offshore and poleward flow, respectively, are shaded. Equatorward flow has negative sign, speeds are cm s^{-1}. Source: Mittelstaedt et al. 1975.

Exceptions that Prove the Rule

Two regions of upwelling and high productivity that are not located along the eastern boundaries of the oceans (i.e., off the west coasts of the continents) are the northwestern Indian Ocean and the equatorial regions. Vigorous upwelling occurs off the east coast of Somalia and Saudi Arabia. During May to September the southwest monsoon blows from the southwest (the condition implied in Figure 1), nearly parallel to the coastline, causing a large transport of surface water (Ekman transport) away from the coast. Just off Saudi Arabia, the sea surface temperature may drop to 18°C while temperatures 1000 km to the east are nearly 30°C. Off Somalia, only nine degrees of latitude from the equator, where the Somali current (the Indian Ocean analog to the Gulf Stream) separates from the coast in a process that enhances upwelling near the coast, the sea surface temperature may be less than 15°C. During the winter the winds blow in the opposite direction, and neither upwelling nor the Somali current is present.

Another region which conspicuously exhibits the effects of upwelling is the eastern equatorial Pacific. Like the coastal upwelling regions, the equatorial regions are characterized by green water and an abundance of fish, which is a sharp contrast to the desert-like regions to the north and south of the mid-ocean equatorial region. The green water is the result of an abundance of phytoplankton: equatorial waters have a high productivity exceeded only in coastal upwelling regions.

Sea surface temperatures in the eastern equatorial Pacific, west of the Galapagos, are lower than temperatures found within 2000 km north or south of the equator, and in July and August sea surface temperatures dip below 20°C at the Galapagos Islands. Upwelling at the equator results from a wind-induced divergence of the surface layer—similar to that in coastal upwelling. The trade winds in equatorial regions blow with a component from the east. Surface water is transported away from the equator immediately north and south of it, the Ekman transport is to the right of the wind in the Northern Hemisphere and to the left of the wind in the Southern Hemisphere. This wind-induced divergence in the surface layer results in upwelling near the equator, with the concomitant cool temperatures and nutrient-rich water.

A Comparison of the Simple Model with Observations

The conceptual model of coastal upwelling presented in the previous sections actually stems from McEwen's (1912) application of Ekman's results to explain ocean temperatures along the west coast of North America. The model continues to be the basis for most contemporary models of coastal upwelling (e.g. O'Brien et al., 1977). Briefly restated, the offshore-directed Ekman transport ($\tau_y f^{-1}$) in the surface layer at the seaward edge of the coastal zone drives coastal upwelling by requiring water inshore to upwell into the surface layer to satisfy continuity. Horizontal flow beneath the surface layer must be convergent to balance the divergence in it caused by the Ekman transport of water away from the coast. This can be done simply, but not necessarily, by cross-shelf flow beneath the surface layer equal and opposite to the Ekman transport in it. Observations from moored arrays of current meters and anemometers can provide a test of the conceptual model.

During the Coastal Upwelling Ecosystems Analysis program (CUEA) three different coastal upwelling regions were intensively studied: Oregon, the CUE-2 experiment, July-August 1973; northwest Africa, the JOINT-1 experiment, March-April 1974; and Peru, the JOINT-2 experiment, March-May 1977. The regions differed in latitude, stratification, and strength and variability of the wind driving the upwelling (Table 1), as well as bathymetry of the shelf and slope (Figure 11). For several weeks during each experiment, moored, fixed-level, current meters recorded horizontal flow in the water column at a midshelf site near the seaward edge of the upwelling zone, and nearby meteorological buoys measured wind. Descriptions and

Table 1. Comparison of three upwelling regions (see Figure 12). τ_y: Mean $\pm$ standard deviation of the alongshore (equatorward) component of the wind stress (dynes cm^{-2}) and maximum/minimum values during the experiments; $\Delta\rho$: Density difference (sigma-t) from surface to bottom at midshelf; R: estimated baroclinic radius of deformation (km).

		τ_y	$\Delta\rho$	R
Oregon (45°N)	0.50±0.73;	3.48/-1.10	2.0	14
Northwest Africa (21°40°N)	1.50±0.93;	3.20/-0.50	0.3	10
Peru (15°S)	0.55±0.35;	1.53/ 0.08	0.5	20

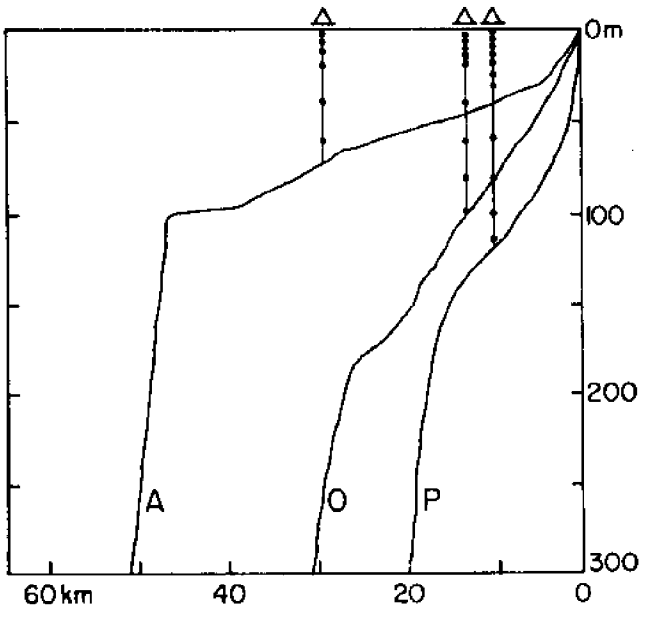

Figure 11. Shelf and slope topography off northwest Africa (21°40'N), Oregon (45°N), and Peru (15°S) with location of moored current meters during CUEA experiments.

analyses of these measurements were published in Halpern (1976); Halpern, Smith, and Mittelstaedt (1978); Brink, Halpern, and Smith (1980); and Smith (1981).

The mean alongshore component of wind stress (Table 1) was favorable in the three regions studied (i.e., the wind blew equatorward along those eastern boundaries). The values for R estimated from the parameters given in Table 1, using $N^2 = g\Delta\rho\, H^{-1}\, \rho^{-1}$, and the hydrographic and biological evidence (Smith, 1974; Huyer, 1976; Huntsman and Barber, 1977; and Brink et al., 1981) support the assumption that the moored arrays in Figure 11 are near the seaward edge of the upwelling zone.

Mean horizontal velocity profiles from these moorings are shown in Figure 12. The alongshore/onshore directions are positive equatorward/eastward—i.e., toward the south and east for Oregon and northwest Africa, and toward the northwest (315°T)/northeast (45°T) for Peru—which are consistent with the general trends of the coastline. Near the surface mean flow is strongly equatorward, as is the wind. The poleward undercurrent is evident on the Oregon and Peruvian shelves, but not on the northwest Africa shelf; a strong poleward undercurrent does exist over the slope off northwest Africa (Figure 9). It is clear from Figure 12 that the mean profile is consistent with the conceptual model of coastal upwelling: offshore flow in a surface layer on the order of 20 to 40 m depth at midshelf causes upwelling of water, supplied by onshore flow in the deeper water, into the surface zone inshore. Whether there exists a quantitative agreement between Ekman transport ($\tau_y f^{-1}$), the offshore transport in the surface layer, and the onshore transport beneath, will be discussed later.

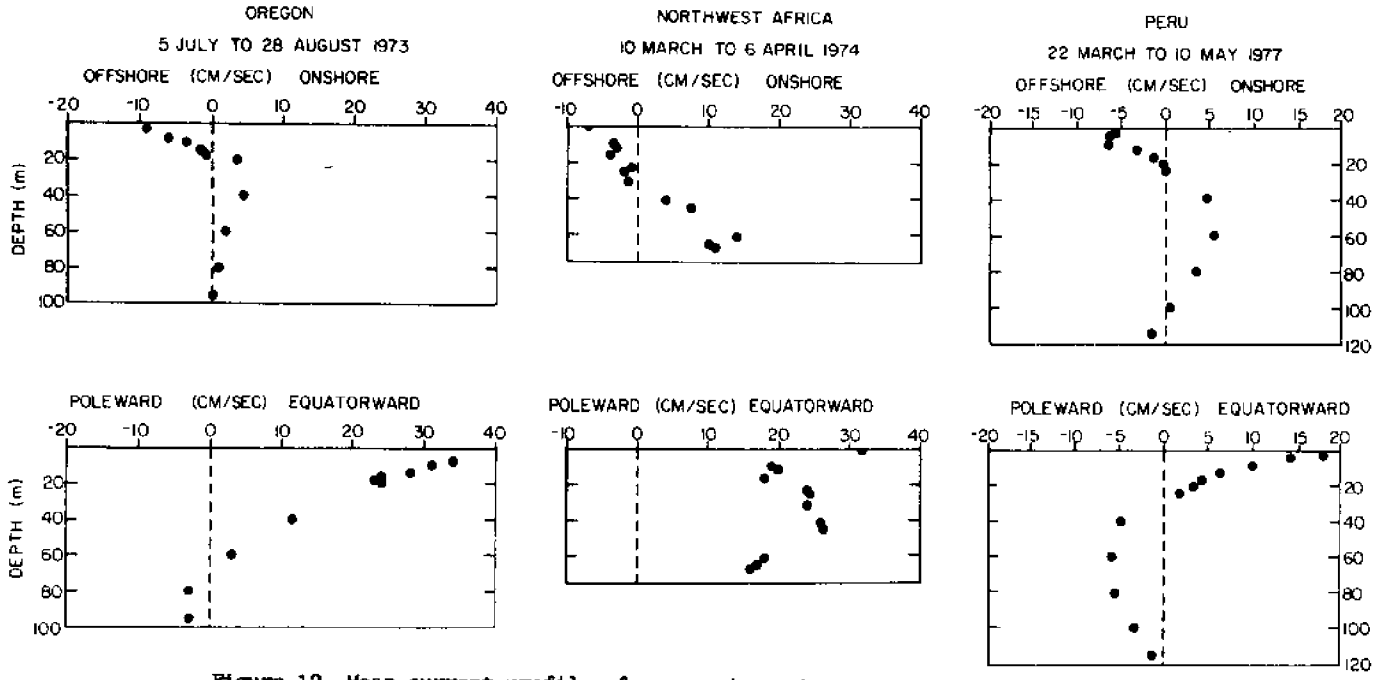

Figure 12. Mean current profiles from moorings shown in Figure 11. Reference: Smith, 1981.

The layer of mean offshore-directed flow is relatively thin: less than 20 m off Oregon, 35 m off northwest Africa and about 30 m off Peru. Recall that the Ekman depth, a measure of the thickness of the Ekman layer, is $D = (2A\, f^{-1})^{1/2}$ where A is the vertical eddy viscosity. Halpern (1976 and 1977) and Brink et al. (1980) estimated A by matching wind stress to near-surface stress due to vertical shear in the alongshore current, $\tau_y = A\, \partial v/\partial z$. Average values for A during periods of strong upwelling favorable winds are 55 $cm^2\ s^{-1}$ and 70 $cm^2\ s^{-1}$ for Oregon, northwest Africa, and Peru; the corresponding Ekman depths are 10 m, 22 m, and 19 m. An alternate estimate of the thickness of the surface layer comes from studies of turbulent boundary layers. Pollard, Rhines, and Thompson (1973) gave the thickness of the surface mixed layer as $D_s = 1.7\, u_* (fN)^{-1/2}$ where u_* is the friction velocity defined by $\tau = \rho u_*^2$. Using the parameters given in Table 1, and estimating mean N^2 as above, D_s = 10 m, 35 m, and 26 m for Oregon, northwest Africa, and Peru respectively. These values agree with the observed thickness of the mean offshore flow layer.

Onshore flow below the surface layer, which could compensate for the upwelling inshore into the offshore flowing surface layer, is clearly not in a bottom Ekman layer off Oregon and Peru. There, deeper flow at midshelf is poleward, and thus the bottom Ekman transport would be directed offshore. Onshore compensatory flow is shallow and is presumably in geostrophic balance with the alongshore pressure gradient. A mean alongshore pressure gradient caused by an alongshore (equatorward) rise of sea level of 1 cm in 100 km would be sufficient to allow a

mean geostrophic onshore flow to balance the mean offshore Ekman transport. Although such a mechanism is utilized in several theories and numerical models, the smallness of the pressure gradient has generally precluded experimental verification.

Off northwest Africa, onshore flow is adjacent to the bottom and its thickness is consistent with a bottom Ekman layer. On the basis of boundary layer theory, the bottom Ekman layer thickness is often assumed to be $D_B = 0.3\ u_* f^{-1}$, where u_* is friction velocity; u_* is estimated as $0.03\ V_g$, where V_g is the "geostrophic speed," or speed outside the boundary layer. (See Weatherly and Martin, 1978, for a discussion of the dynamics of the oceanic bottom boundary layers and especially the effect of stratification, which causes the above expression for D_B to overestimate thickness—perhaps by as much as a factor of 3 off Oregon, but less off northwest Africa). For northwest Africa V_g is taken to be the maximum vector mean speed beneath the surface Ekman layer, viz. $V(45\ m) = 28\ cm\ s^{-1}$. This yields $D_B = 64$ m and suggests that the bottom Ekman layer does play an important, perhaps dominant, role in upwelling circulation. For comparison, D_B is computed for Oregon and Peru, using a more directly determined estimate of $u_* \sim 0.42\ cm\ s^{-1}$ off Oregon (Caldwell and Chriss, 1979) and estimating u_* for Peru as it was for northwest Africa, using $V\ (59\ m) = V_g = 12\ cm\ s^{-1}$. The result is $D_B = 16$ m off Oregon and 38 m off Peru. These estimates of D_B are consistent with mean velocity profiles and suggest that an Ekman bottom layer provides the compensatory onshore flow off northwest Africa, but plays a minor role—and an opposite one, because of the mean poleward flow—off Peru and Oregon.

Upwelling Events

So far upwelling has been discussed in terms of mean or climatological features, causes, and effects. In Figure 1, distribution of half the world fisheries reflected a possible adjustment of the ecosystem on the evolutionary time scale. In Figure 3 climatological winds were compared to average temperature differences between the coast and mid-ocean. The patterns agreed well with what would be expected from the conceptual model, which explained costal upwelling as a response to local winds. But winds fluctuate on many time scales. Does coastal upwelling? The term "upwelling events"—denoting periods of strong upwelling associated with stronger-than-average, upwelling-favorable, alongshore winds—is now a common expression in the literature. Let us look at the changes corresponding to the several-day fluctuations in atmospheric circulation, i.e., the fluctuations that make up our "weather."

The Oregon coast is a good place to see the effects of variable winds on coastal upwelling. Although winds are generally favorable for upwelling from April through September, occasional storms or the passage of low pressure systems cause winds to blow from the southwest. Winds from the south or southwest cause an Ekman transport toward the coast. The wind, measured at the coast near Newport (45^{O}N) during August 1972, are shown in Figure 13. During some of these weeks an aircraft with infrared thermometry equipment flew over the coastal waters (O'Brien, 1972): sea surface temperature maps from five flights are shown. Winds had been favorable for coastal upwelling (from the north) in early August, and the SST (sea surface temperature) map for 10 August 1972 shows cold water everywhere. The winds then became southerly (from the south) on 12 August, and warmer water covered the region by 17 August. Within two days (24 August) after the wind again shifted to northerly, cold water began outcropping nearshore. Strong upwelling-favorable winds continued, and on 30 August cold water was again found everywhere in the coastal region—the warmer surface water having been pushed further out to sea.

Periods of intensified upwelling-favorable winds are called upwelling wind events. The duration and intensity of events vary from region to region, and some biologists think various upwelling ecosystems may have evolved to take advantage of such characteristics. Weak winds between events and stable stratification resulting from warmer water developing over cold water allow phytoplankton populations to bloom and take full advantage of the burst of nutrients supplied during the windy event.

Both the higher trophic levels of the marine food chain and man do take

Figure 13. Sea surface temperature maps from the Oregon coastal upwelling region. Daily average wind vectors, at Newport, are shown for an upwelling event cycle. Sea surface temperatures demonstrate the rapid response of the coastal upwelling process to wind fluctuations. Source: O'Brien, 1972.

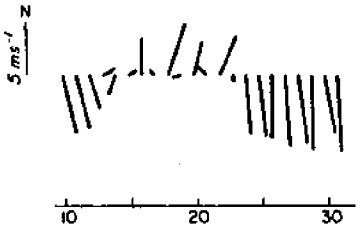

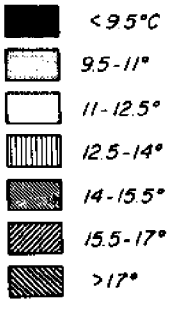

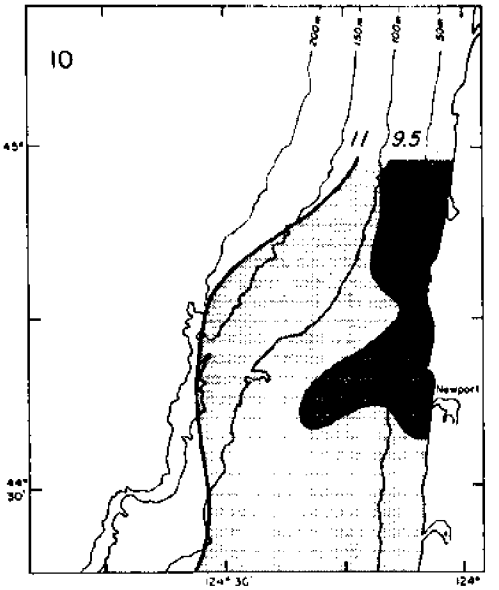

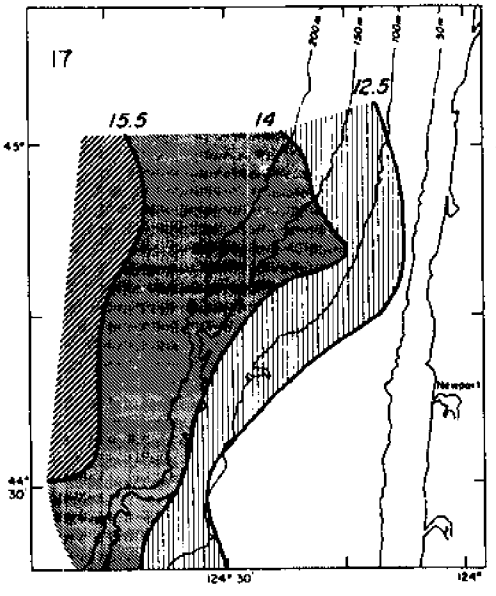

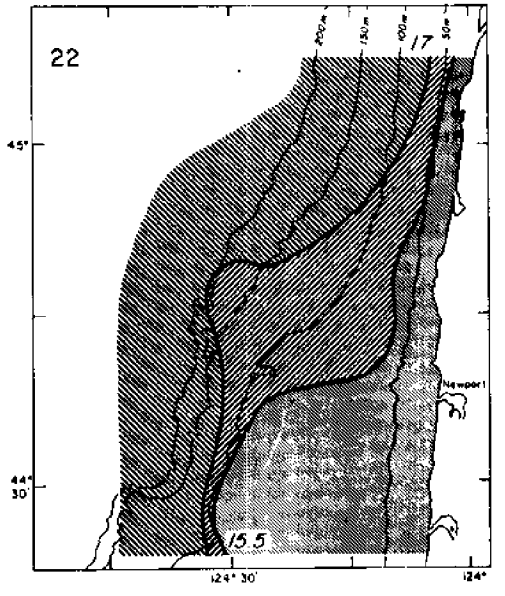

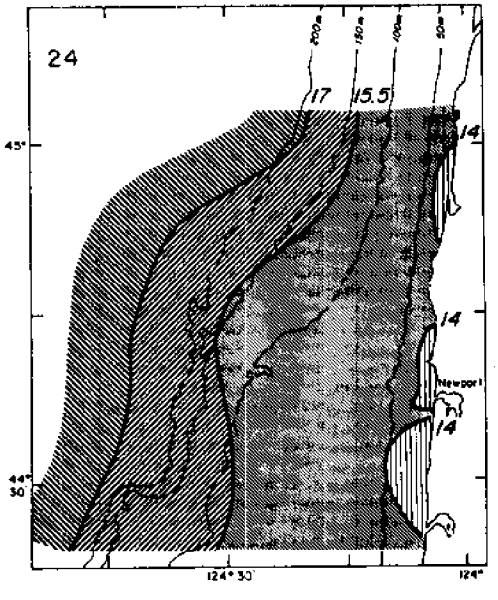

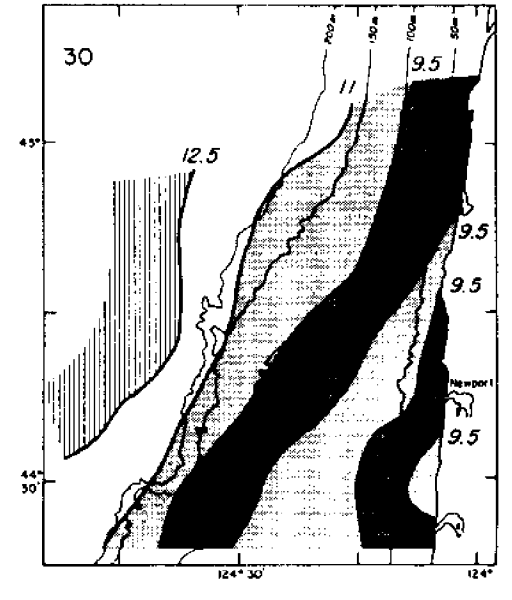

advantage of the temperature distributions seen in Figure 13. The highest concentrations of phytoplankton and zooplankton are frequently found near the boundary between cold, nutrient-rich, upwelled water and warmer surface water of the offshore ocean. (Sharp boundaries are called fronts, analogous to the fronts in meteorology that separate air masses of differing densities.) The coho salmon of the Pacific Northwest coast prefer temperatures between 11°C and 14°C, intermediate between the offshore ocean water (15° to 17°C) and nearly upwelling water at the coast (8° to 10°C). This is where fishermen are most likely to find a good catch, and the fishermen of Oregon have long used thermometers to guide their fishing.

Detailed knowledge of mixing and the true trajectories of water in response to wind is limited, but differences in productivity among several upwelling regions may be partly explained by differences in the strength and duration of wind events. For example, off northwest Africa the winds at times blow very strongly (Barton et al., 1977), perhaps flushing out the region's waters by dispersing the contents of the surface layer before phytoplankton populations can build up. Perhaps, too, the vigor of the surface flow removes the plankton offshore beyond the undercurrent, reducing the efficiency of the conveyer belt. Often, in response to strong winds, a deep and well-mixed surface layer develops, which mixes phytoplankton below where they receive sufficient light for photosynthesis. Strong upwelling-favorable winds can perhaps be too strong for high primary productivity to be achieved.

Since "upwelling events" are important and ubiquitous and the standard deviation of alongshore wind stress is not negligible (Table 1), we may well ask if the mean profiles shown in Figure 12 are meaningful. Could it be that they simply show an arithmetic mean, never realized in nature, between two extreme states--upwelling events and quiescent periods? To compare the "event" flow pattern to the mean we chose the wind event associated with the maximum wind stress in Table 1. Profiles of cross-shelf flow (Figure 14) show the low-pass filtered data at a time when wind stress was greater than the mean for more than one inertial period, the characteristic time scale for Ekman layer "spin-up." The σ_t or temperature profiles taken before the wind intensified and after it peaked, indicate that water properties changed, which would expected during an "upwelling event." The close similarity of onshore/offshore circulation at the height of upwelling to the mean profile is clear. Even off Oregon, where the standard deviation of wind stress is greater than the mean, and wind stress during the event is almost an order of magnitude greater than the mean, the event and mean profiles are very similar. Therefore, the conceptual model of upwelling holds both in the mean and during "upwelling events."

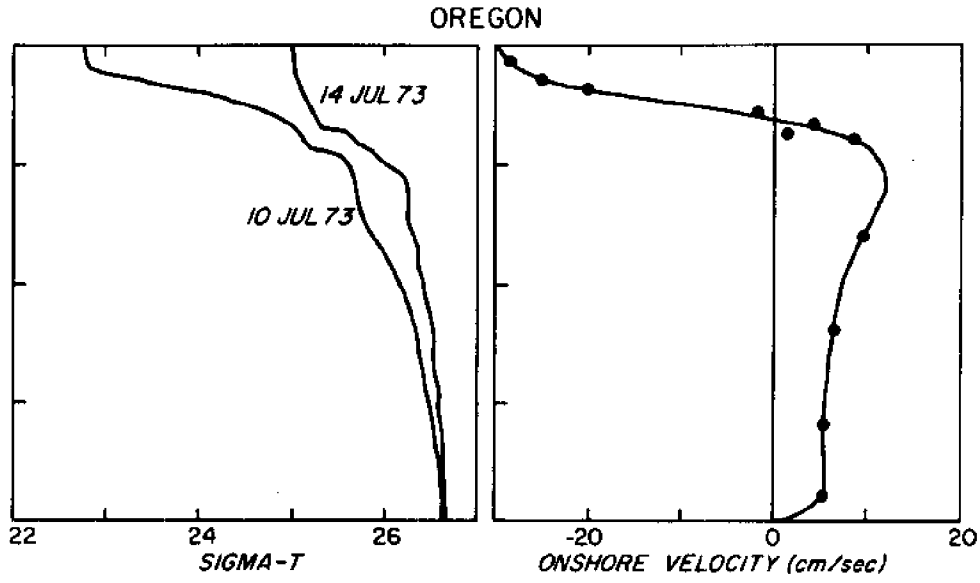

Figure 14. Vertical profiles of Sigma-t (density) or temperature before and during an upwelling event, and cross-shelf flow at the peak of the event (3 April 1974, 12 July 1973, and 9 April 1977 respectively). Source: Smith, 1981.

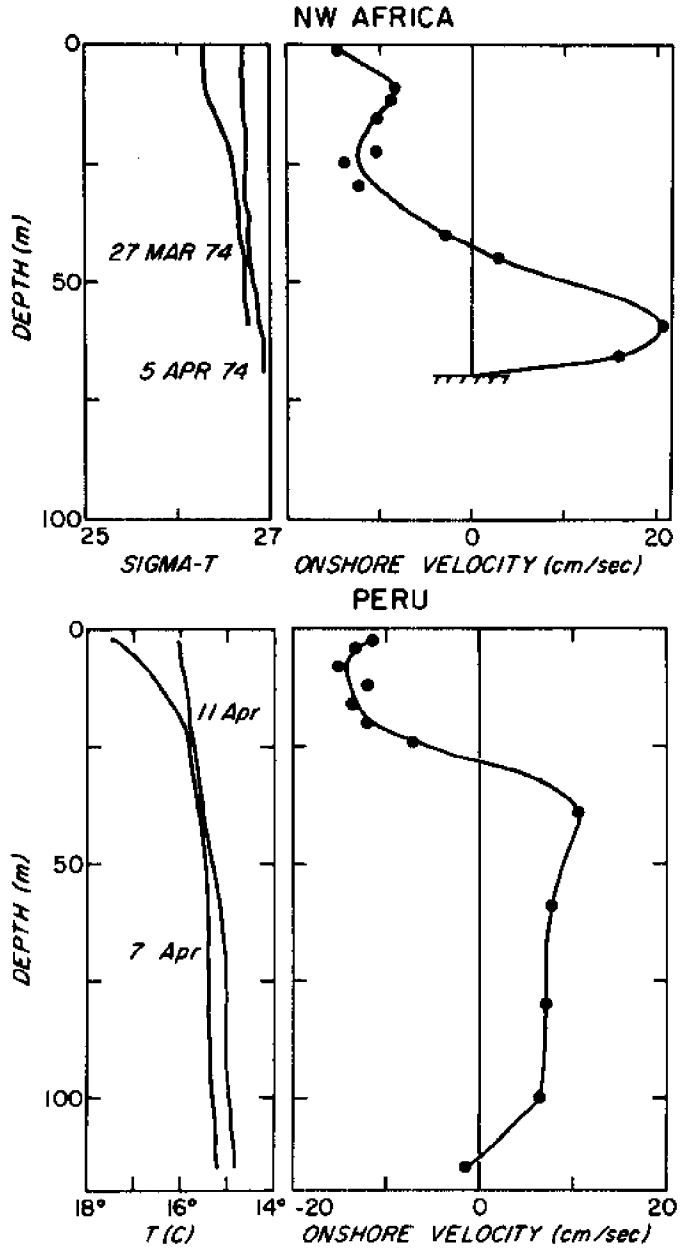

A Quantitative Test

Quantitative estimates of the amount of water upwelling are needed to estimate nutrient fluxes and to compare the temporal and spatial variations in the "efficiency" of upwelling regimes. Unfortunately, the small vertical velocities (at most 10^{-2} cm sec^{-1}) can barely be measured at all, and certainly not with the temporal and spatial coverage necessary to provide useful estimates. From horizontal velocities measured by moored current meters, the divergence in the horizontal velocity field between the coast and some offshore location can be inferred, and hence the amount of water that must upwell to satisfy continuity.

Water velocity measurements, however, are generally difficult and always expensive to obtain, and are inevitably spatially insufficient. On the other hand, wind—at least on the coast—is relatively easy to measure. Important questions, answered in part during CUEA and being addressed with the data from more extensive and sophisticated instrumentation used during CODE (Coastal Ocean Dynamics Experiment) off California in 1981 and 1982, are the following:

- Is the observed cross-shelf transport in the surface layer, $U_S = \int_{-D}^{0} u\,dz$, in quantitative agreement with the Ekman volume transport, $\tau_y(\rho f)^{-1}$, computed from the wind observations?
- Is the offshore flow, U_S, balanced by an equal onshore flow below, $U_L = \int_{-b}^{-D} u\,dz$, or is the upwelling process more complex?

The second question can be restated: Is the convergence in the flow required to balance the Ekman layer divergence, caused by wind stress along the coastal boundary, two-dimensional ($\frac{\partial u}{\partial x} + \frac{\partial w}{\partial z} = 0$), involving only the cross-shelf (u) and vertical (w) velocity field, or three-dimensional ($\frac{\partial u}{\partial x} + \frac{\partial v}{\partial y} + \frac{\partial w}{\partial z} = 0$)? If the latter, then variations in upwelling intensity along the coast are likely, independent of variations in wind. Since wind is highly variable, the questions may have different answers with respect to the mean circulation than on the time scale of upwelling events.

Definition of the alongshore/onshore coordinate system is crucial in tests of volume flux balances since both mean and variable alongshore flows are much greater than cross-shelf flow. Net alongshore transports are nearly an order of magnitude greater than offshore/onshore transports or theoretical Ekman transports. Thus, a

slight rotation (only a couple degrees) in the nominal alongshore/onshore coordinate system can make an appreciable difference in cross-shelf transport. The local isobath direction is the natural alongshore direction in coastal upwelling through continuity, and in time-dependent inviscid models, variability in alongshore flow (v) results from the $\frac{\partial v}{\partial t}$ + fu balance (Allen, 1980). In a stratified fluid, the flow tends to organize in the along-isobath direction, and the CUEA results (e.g., Kundu and Allen, 1976) clearly show the tendency for the horizontal velocity fluctuations to align along isobaths.

In general, bathymetric charts are not precise enough to allow estimates of isobath directions to within a few degrees. Furthermore, it is not apparent over what spatial scale directions of the wiggling and curving isobaths should be estimated. In this paper, the major principal axis of the total volume transport vector (velocity integrated from the bottom, z = -b, to the surface, z = 0: $U = \int_{-b}^{0} u dz$, $V = \int_{-b}^{0} v dz$) is chosen as an objective definition of alongshore direction, i.e., the direction of maximum variance of the depth-averaged velocity field is assumed to be the "alongshore" direction. These directions agree well with isobath directions. A beneficial corollary is that cross-shelf fluctuations are, by definition, uncorrelated (at 0 lag) with alongshore fluctuations in the principal axis system. Thus, cross-shelf transports are not "contaminated" with an alongshore transport contribution.

Volume transports were computed by numerical (trapezoidal) integration of the vertical array of velocity measurements at depths indicated in Figure 11. Contributions to integration from current meters above and below a fixed depth D were assigned to the upper and lower layers respectively. D was taken to be the depth midway between the deepest current meter showing offshore flow and the next current meter deeper.

The mean Ekman transport computed from wind stress and measured mean transports in the upper and lower layers are given in the transport principal axis system in Table 2. (For comparison, cross-shelf transport in the surface layer is also shown for the coordinate system defined by zero mean, net cross-shelf transport.) The large mean onshore transport, U_L, in the lower layer off Oregon is probably real and results from a positive mean $\partial v/\partial y$: the mean southward flow along the 100 m isobath increases by about 2.5 cm s^{-1} from mooring C (used in this paper) to mooring P, about 50 km southward (see figures and statistics in Kundu and Allen, 1976). Increased onshore flow between C and P of nearly 1 cm s^{-1} would be required to supply the estimated increased transport over the 50 percent wider shelf inshore of 100 m at P. Thus about 100 units of the lower layer onshore

Table 2. Mean Ekman transport computed from the alongshore component of the wind stress, mean measured cross-shelf transport in the surface (U_S) and lower (U_L) layers (principal axis system), and the magnitude of the offshore/onshore transport in the upper/lower layer in the zero net cross-shelf transport coordinate system, i.e., the latter assumes two-dimensional upwelling. Transport is given in 10^2 cm^3/cm sec, and is positive directed onshore. From Smith, 1981.

	$\tau_y/\rho f$	U_S	U_L	$\lvert U_o \rvert$
Oregon	- 48±69	- 65±109	198±177	143
Northwest Africa	-274±170	-145±184	248±160	195
Peru	-141± 89	- 82±148	120±260	90

transport off Oregon (Table 2) may be the result of a mean $\partial v/\partial y$ and not be part of the compensatory flow for the mean offshore Ekman transport.

If this is the case, the Oregon lower layer transport would not appear anomalously large relative to the Ekman transport. A non-negligible mean $\partial v/\partial y$ may be ubiquitous in coastal upwelling regions as a result of bathymetric variations and thus preclude a mean two-dimensional mass balance except over space scales that are large compared to bathymetric variations.

The observed mean offshore transport is in fair agreement with the deviations in closer agreement. Does the Ekman relation hold for the variable flow? To test this, the correlations of the U_S series against the $\tau_y\ (\rho f)^{-1}$ series, with the means removed, were computed. The maximum correlations, all significant at greater than 99.9 percent level of significance, are 0.66 with U_S lagging τ_y by six hours off Oregon; 0.71 with 0 lag off northwest Africa, 0.54 with U_S lagging τ_y by six hours off Peru. A quantitative answer to the question is provided by the linear regression of U_S on $\tau_y(\rho f)^{-1}$, with U_S series lagged to provide the maximum correlation. The regression coefficient is unity to within the standard error in all cases (Table 3), i.e., the observed surface layer cross-shelf transport variations agree with those predicted from wind stress using simple Ekman theory.

The lower layer transports, U_L, were also significantly correlated with $\tau_y(\rho f)^{-1}$ (at the 99 percent significance level) but the regression coefficients were not unity to within the standard error except for Oregon. The results are also shown in Table 3. The cross correlation between U_S and U_L were considerably poorer than between τ_y and either U_S or U_L. Only for northwest Africa and Peru were the correlations significantly different from zero at the 90 percent level (northwest Africa was -0.39 with U_L lagging U_S by 36 hours; Peru was -0.40 with U_L lagging U_S by 48 hours). The negligible correlation between U_S and U_L off Oregon may be the

Table 3. Coefficients from linear regression of measured cross-shelf transport in the surface layer, U_S, and lower layer, U_L, on the Ekman transport computed from wind measurements. (U positive onshore, τ_y positive equatorward alongshore). From Smith, 1981.

	Dependent Variable	Correlation Coefficient	Regression Coefficient ± Standard Error
Oregon	U_S	-0.66	-1.04±0.33
	U_L	0.49	1.25±0.54
Northwest Africa	U_S	-0.71	-0.77±0.30
	U_L	0.64	0.64±0.25
Peru	U_S	-0.51	-0.84±0.33
	U_L	0.63	1.85±0.36

result of energetic, barotropic, continental shelf waves, which are present in the Oregon data (Cutchin and Smith, 1973), obscuring the "baroclinic" cross-shelf circulation response to upwelling. In any case, the U_L, U_S relation cannot be characterized by a two-dimensional mass balance on the event time scale in any region. In nature, two-dimensional upwelling circulation seems to be ephemeral, and it should be no surprise to observe "upwelling centers," the spatial counterpart to "upwelling events." Topographic effects may easily cause $\frac{\partial v}{\partial y}$ to be non-zero and hence local upwelling ($\frac{\partial w}{\partial z}$) not to balance exactly the offshore Ekman transport. Nevertheless, simple Ekman dynamics does seem to hold reasonably well for the surface layer in the mean and on the event time scale. An "upwelling index" based on wind stress should have quantitative efficacy for scales that are large compared to upwelling centers (>>10 km).

Epilogue

Coastal upwelling studies of the 1970s focused on relatively small subregions of major coastal upwelling regions extending along the west coasts of the United States, northwest Africa (Senegal, Mauritania, and Morocco,) and Peru. Our understanding of the coastal upwelling process on time scales of days to a few months (the typical duration of an experiment or expedition) and on a local space scale (the order of 20 km alongshore and, perhaps, 100 km offshore—the area within which a ship can make repeated daily measurements) is much improved over a decade earlier; or, at least, much work and thought has been expended (e.g., see an attempt at synthesis of the studies in Barber and Smith, 1981). These localized (in space and time) studies, because they were made within persistent, large-scale, coastal upwelling systems, emphasized the significance of both spatial inhomogeneity and interannual variability, which are part of the coastal upwelling process. These topics will, I hope, be more adequately addressed in the 1980s, and I will comment briefly on them.

The apparent spatial inhomogeneity of coastal upwelling can be seen off Peru in Figure 15, and on a somewhat larger scale in Figure 3 and Figure 4. As stated earlier, these upwelling centers can be considered the spatial analogy to the temporal upwelling events. The wind field is of course not uniform along upwelling

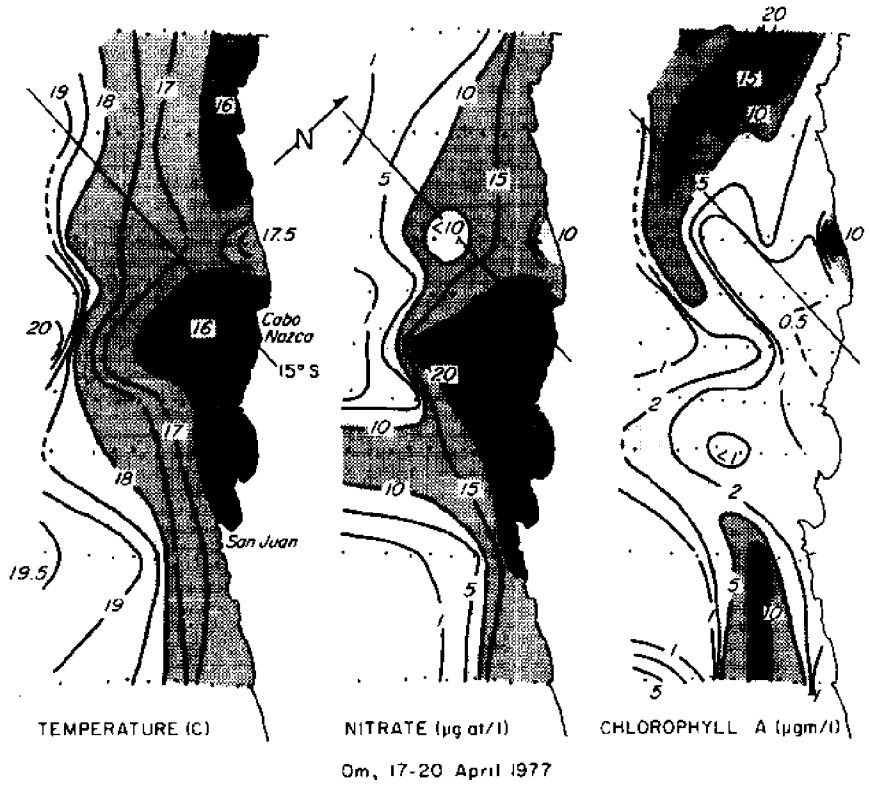

Figure 15. Sea surface temperature (SST), nitrate, and chlorophyll maps off Peru.

coasts; Figure 16 shows both the latitudinal and seasonal variability off North America. Thus, one should expect the Ekman transport and resulting coastal upwelling to vary. It is also well known, both from observations and theory, that upwelling intensifies equatorward of capes. This is a consequence of the enforced curvature of the horizontal flow (Arthur, 1965). Note the SST patterns near Cap Blanc (Figure 3) and Cabo Nazca (Figure 15).

Even without variations in wind and coastline one might expect variations in upwelling (Preller and O'Brien, 1980). If the offshore Ekman transport in the surface layer remains unchanged, variations in the alongshore flow, caused by variations in the bottom topography, could induce variations in vertical flow. In other words, an alongshore convergence (or divergence) could reduce (or increase) the amount of upwelling needed to compensate for the offshore Ekman transport. The results in the previous section strongly suggest that the $\frac{\partial v}{\partial y}$, i.e., the alongshore convergence, cannot be neglected.

Wind and the weather may differ from year to year, so may the amount of upwelling. One might infer that years with strong upwelling would be followed by good fishing years: the reproductive success and survival of the young would be enhanced by the abundance of food in good upwelling years, leading to good fishing in a later year. Some species off Oregon (bottomfish, shrimp, etc.) depend on the

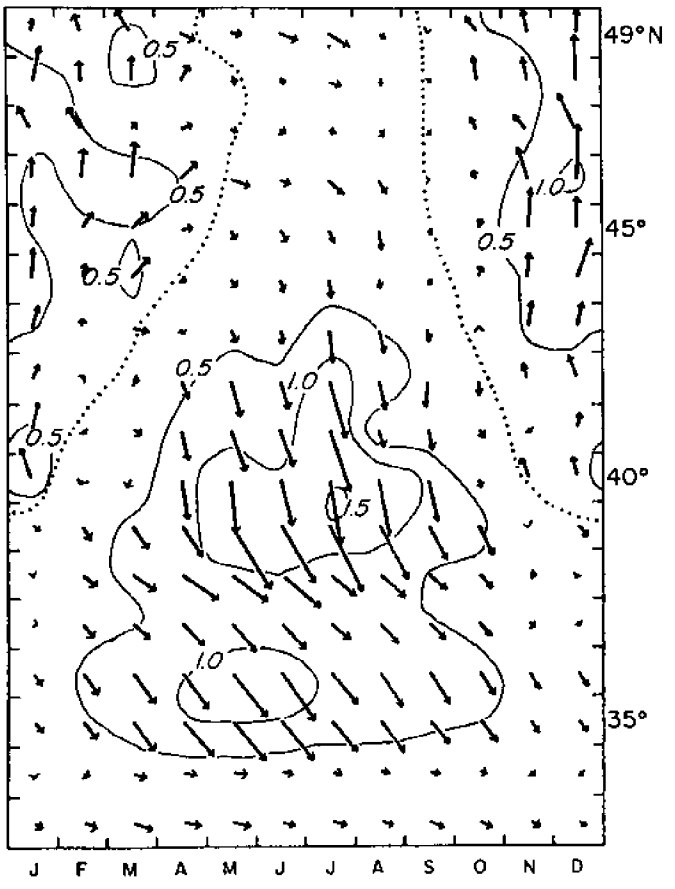

Figure 16. Long-term, mean monthly wind stress for one-degree squares along the west coast of the United States, computed from ship reports from 1857-1972. Vectors show direction and magnitude of monthly mean stress at each latitude. The dotted line shows the boundary between stress vectors with a southward component and those with a northward component. Magnitude of stress is contoured at intervals of 0.5 dynes/cm^2. Source: Nelson, 1977.

increased food availability during summer upwelling for their growth and survival (cf. Peterson, 1973). It should be noted that off Oregon (45°N), the winds have a strong seasonal cycle (cf. Figure 16). A very early or late onset to the upwelling season (southward winds) might have a profound influence on the reproductive success of some species, even though the total amount of upwelling during the subsequent season might be normal.

In contrast to Oregon, the winds off central Peru (15°S) are always equatorward (upwelling favorable) with seldom a single day of poleward winds. The contrast is apparent in the annual statistics for the years during which the intensive CUEA experiments took place off Oregon (1973) and Peru (1976-7). Off Oregon, the annual mean wind stress is actually unfavorable for upwelling, due to the predominant strength of winter storms which causes poleward winds, and is 0.16 dynes/cm^2 poleward with a standard deviation of 0.81 dynes/cm^2. Off Peru the annual mean is 0.88 dynes/cm^2 equatorward (favorable for upwelling) with a standard deviation of only 0.44 dynes/cm^2. Nevertheless, one of the most dramatic examples of the impact of an oceanographic phenomenon on man's social and economic fabric occurs in the Peruvian coastal upwelling region. Coastal upwelling along Peru's coast supported the world's largest fishery: the Peruvian anchoveta fishery in 1972 accounted for 22 percent of all the fish caught throughout the world. The anchoveta finds its way to the world economic stage as fish meal, which is sold in North America and Europe as feed supplement for poultry, hogs, and cattle.

Long before man began to manufacture fish meal, Guano birds, feeding on the rich anchoveta stocks off Peru, provided the basis for a guano (fertilizer) industry. The Incas used guano to fertilize the barren soil of Peru; intense commercial mining of guano deposits began in the latter half of the nineteenth century.

After World War II, fishermen began to compete with guano birds for a share of the anchoveta stocks. The fishery developed rapidly in the 1950s (see Figure 17) and dominated the feed supplement markets in the 1960s and early 1970s. By 1972, two-thirds of the fish meal entering international trade was from Peru.

Today, the anchoveta fishery is in danger of complete collapse. Overfishing may have put it in jeopardy, but an environmental perturbation called El Niño may have dealt its death-blow. El Niño is the occasional appearance of excessively warm water along the coast of Peru, which tends to coincide with the Christmas season (hence the name) and the Southern Hemisphere summer. This is the season when trade winds offshore and coastal winds off northern Peru (5°S) are slightly weaker and equatorial water flows south (poleward). At times, abnormally warm

water persists for many months and affects much of Peru's coast, causing the anchoveta to either disappear or move to deep water where they are out of reach of both fishermen and birds. Note the correlation between anchoveta catch and temperature in Figure 17. The temperature (SST) anomalies observed at the Galapagos Islands occur all along the Peru coast (Enfield and Allen, 1980).

In 1965, in 1972-73, and in 1976-77, there were severe El Niños. The one in 1972-73, came after years of sustained high production of fish meal from the anchoveta fishery, and eliminated almost half of the feed supplement sources for livestock, driving up the cost of soybeans (a substitute source of feed supplement) and, of course, poultry and meat (see Figure 17). The anchoveta fishery did not recover as after previous El Niños. Ominously, there was another reproductive failure associated with the 1976 El Niño. The statistics for 1977 were even poorer than 1973. Heavy fishing coupled with environmental catastrophes of 1972-73 and 1976 reduced the fishery from the world's largest to insignificance in a few years.

What causes El Niño? It had once been thought that El Niño was due to weak local winds resulting in weak coastal upwelling. This is not the case and, indeed, coastal winds at Callao (12^{o}S) are actually more strongly favorable for upwelling during El Niño (Enfield, 1981). Wyrtki (1975) proposed a theory that El Niño is the dynamic response of the equatorial part of the Pacific Ocean to atmospheric forcing. During prolonged, excessively strong, southeast trade winds in the eastern tropical Pacific, warm water is "piled up" in the western Pacific. El Niño results from the reaction of the equatorial Pacific to the relaxation of the southeast trades back to normal or below normal strength. The water from the western Pacific "sloshes" back when the trades relax and this leads to a deepening of the surface layer (with its warm, nutrient-poor water) off Ecuador and Peru. Local coastal upwelling still continues, but instead of drawing cool, nutrient-rich water to the surface, the upwelling process doesn't reach below the now deeper surface layer of warm, nutrient-poor water. The nutrient-rich water is out of reach--like the anchovies.

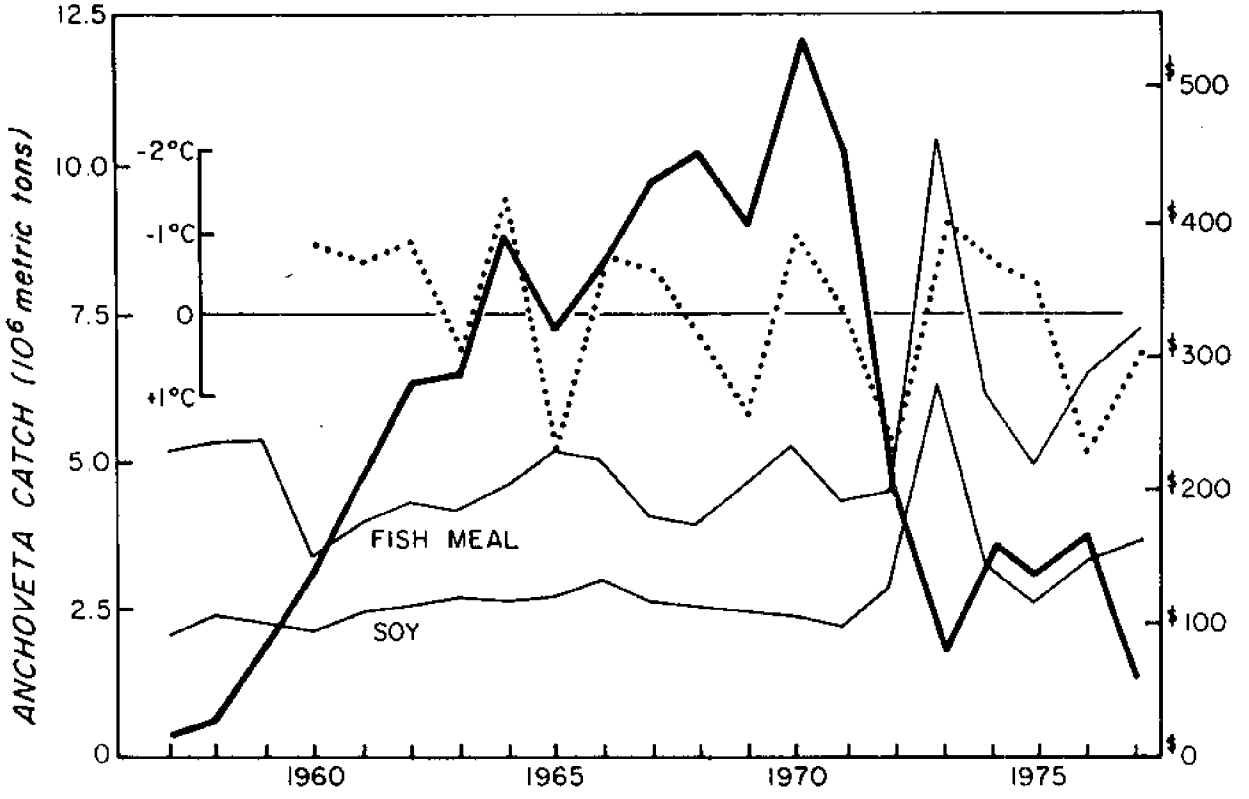

Figure 17. Galapagos Islands SST, anchoveta catch and soy bean prices. Large-scale commercial exploitation of the fishery developed in the 1950s, reached a peak in 1970, and faltered after El Niño of 1972. The heavy solid line represents the annual sea surface temperature anomaly at Baltra; the light solid lines represent the cost of soybean and fish meal (in 1972 U.S. dollars per metric ton). The anchoveta catch comes principally from between 6°S and 12°S, and most of it is landed at Chimbote. The sea surface temperature anomaly is relative to the 19-year mean of 23.8°C; the temperature scale is inverted with upward indicating enhanced upwelling, i.e. colder temperatures. Source: R.T. Barber and colleagues. 1979. Biology and eastern equatorial dynamics: A scientific proposal to NSF. (Unpublished manuscript, unfunded proposal. Sic transit gloria mundi).

References

Allen, J.S. 1980. Models of wind-driven currents on the continental shelf. Annual Review of Fluid Mechanics 12:389–433.

Arthur, R.S. 1965. On the calculation of vertical motion in eastern boundary currents from determiniations of horizontal motion. Journal of Geophysical Research 70:2799–2803.

Bakun, A. 1973. NOAA Technical Report NMFS SSRF-671.

Barber, R.T. and R. L. Smith. 1981. Coastal upwelling ecosystems. In A.R. Longhurst, ed., Analysis of Marine Ecosystems. London: Academic Press. 741 pp.

Barton, E.D., A. Huyer, and R. L. Smith. 1977. Temporal variation observed in the hydrographic regime near Cabo Corveiro in the northwest African upwelling region, February to April 1974. Deep-Sea Research 24:7–23.

Brink, K.H., D. Halpern, and R.L. Smith. 1980. Circulation in the Peruvian upwelling system near 15°S. Journal of Geophysical Research 85:4036–4048.

Brink, K.H., B.H. Jones, J.C. Van Leer, C.N.K. Mooers, D.W. Stuart, M.R. Stevenson, R.C. Dugdale, and G.W. Heburn. 1981. Physical and biological structure and variability in an upwelling center off Peru near 15°S during March, 1977. Coastal and Estuarine Sciences 1:473–495.

Brockmann C., E. Fahrbach, A. Huyer, and R.L. Smith. 1980. The poleward undercurrent along the Peru coast: 5 to 15°S. Deep-Sea Research 27:847–856.

Caldwell, D.R. and T. M. Chriss. 1979. The viscous sublayer at the sea floor. Science 206:1131–1132.

Charney, J.G. 1955. The generation of oceanic currents by wind. Journal of Marine Research 14:477–498.

Cutchin, D.L. and R.L. Smith. 1973. Continental shelf waves: low-frequency variations in sea level and currents over the Oregon continental shelf. Journal of Physical Oceanography 3:73–82.

Ekman, V.W. 1905. On the influence of the earth's rotation on ocean currents. Arkiv. Mat. Astron. Fysik 12:1–52.

Enfield, D.B. 1981. Thermally driven wind variability in the planetary boundary layer above Lima, Peru. Journal of Geophysical Research 86:2005–2016.

Enfield, D.B. and J.S. Allen. 1980. On the structure and dynamics of monthly mean sea level anomalies along the Pacific Coast of North and South America. Journal of Physical Oceanography 10:557–578.

Halpern, D. 1976a. Measurements of near-surface wind stress over an upwelling region near the Oregon coast. Journal of Physical Oceanography 6:108–112.

_____. 1976b. Structure of a coastal upwelling event observed off Oregon during July 1973. Deep-Sea Research 23:495–508.

----------1977. Description of wind and of upper ocean current and temperature variations on the continental shelf off northwest Africa during March and April 1974. Journal of Physical Oceanography 7:422-430.

Hickey, B. 1979. The California Current system--hypotheses and facts. Progress in Oceanography 8:191-279.

Huntsman, S.A. and R.T. Barber. 1977. Primary production off northwest Africa: the relationship to wind and nutrient conditions. Deep-Sea Research 24:25-33.

Huyer, A. 1976. A comparison of upwelling events in two locations: Oregon and northwest Africa. Journal of Marine Research 34:531-546.

Kundu, P.K. and J.S. Allen. 1976. Some three-dimensional characteristics of low frequency current fluctuations near the Oregon coast. Journal of Physical Oceanography 6:181-199.

McEwen, G.F. 1912. The distribution of ocean temperatures along the west coast of North America deduced from Ekman's theory of the upwelling of cold water from adjacent ocean depths. Int. Revue. ges. Hydrobiol. Hydrogr. 5:243-286.

Mittelstaedt, E., R.D. Pillsbury, and R.L. Smith. 1975. Flow patterns in the northwest African upwelling area. Deutschen Hydrographischen Zeitschrift 28:145-167.

Mooers, C.N.K., C.A. Collins, and R.L. Smith. 1976. The dynamic structure of the frontal zone in the coastal upwelling region off Oregon. Journal of Physical Oceanography 6:3-21.

National Science Board. 1971. Environmental Science--Challenge for the Seventies. Washington, D.C.: National Science Foundation.

Nelson, C.S. 1977. NOAA Technical Report NMFS SSRF-714.

O'Brien, J.J. 1972. CUE-1 Meteorological Atlas, Volume 1. CUEA Technical Report 11.

O'Brien, J.J., R.M. Clancy, A.J. Clarke, M. Crepon, R. Elsberry, T. Gammelsrød, M. MacVean, L.P. Roed, and J.D. Thompson. 1977. Upwelling in the ocean: two- and three-dimensional models of upper ocean dynamics and variability. In E.B. Kraus, ed., Modelling and Prediction of the Upper Layers of the Ocean. New York: Pergamon.

Peterson, W.T. 1973. Upwelling indices and annual catches of Dungeness crab, Cancer magister, along the west coast of the United States. Fishery Bulletin 71:902-910.

Pollard, R.T., P.B. Rhines, and R.O.R.Y. Thompson. 1973. The deepening of the wind-mixed layer. Geophysical Fluid Dynamics 3:381-404.

Preller, R. and J.J. O'Brien. 1980. The influence of bottom topography on upwelling off Peru. Journal of Physical Oceanography 10:1377-1398.

Ryther, J.H. 1969. Photosynthesis and fish production in the sea. Science 166:72-76.

Smith, R.L. 1974. A description of current, wind, and sea level variations during coastal upwelling off the Oregon coast. Journal of Geophysical Research 79:435–443.

----------. 1978. Les remontees d'eau profonde, source de vie des oceans. La Recherche 9:855–863.

----------. 1981. A comparison of the structure and variability of the flow field in three coastal upwelling regions: Oregon, northwest Africa, and Peru. Coastal and Estuarine Sciences 1:107–118.

Stommel, H. 1960. The Gulf Stream. Berkeley: University of California Press.

Thompson, J.D. 1977. Ocean deserts and ocean oases. In M.N. Glantz, ed., Desertification. Boulder, Colorado: Westview Press.

Turekian, K.K. 1968. Oceans. New York: Prentice-Hall.

Weatherly, G.L. and P.J. Martin. 1978. On the structure and dynamics of the oceanic botton boundary layer. Journal of Physical Oceanography 8:557–570.

Wooster, W.S., A. Bakun, and D.R. McLain. 1976. The seasonal upwelling cycles along the eastern boundary of the North Atlantic. Journal of Marine Research 34:131–141.

Wyrtki, K. 1975. El Nino—the dynamic response of the Pacific Ocean to atmospheric forcing. Journal of Physical Oceanography 5:572–584.

Yoshida, K. 1955. Coastal upwelling off the California coast. Records of Oceanographic Works in Japan 2(2):8–20.